International Journal of Heat and Technology

Vol. 43, No. 1, February, 2025, pp. 161-171

Journal homepage: http://iieta.org/journals/ijht

Effects of Dufour and Radiation on MHD Convective Heat and Mass Transfer in Viscoelastic Fluid Flow Past a Porous Plate



Ananthi Loganathan, Sujatha Elamparithi*

Department of Mathematics, College of Engineering and Technology, SRM Institute of Science and Technology, Kattankulathur 603203, India

Corresponding Author Email: sujathae@srmist.edu.in

Copyright: ©2025 The authors. This article is published by IIETA and is licensed under the CC BY 4.0 license (http://creativecommons.org/licenses/by/4.0/).

https://doi.org/10.18280/ijht.430117

Received: 10 December 2024 Revised: 3 February 2025 Accepted: 18 February 2025 Available online: 28 February 2025

Keywords:

MHD, pressure, chemical reaction, visco-

elastic, Dufour effect

ABSTRACT

The study examines the impact of combined radiation and chemical reaction influences on the MHD free convective heat and mass transfer (HAMT) flow of an incompressible, viscous, electrically conductive elastic fluid via a permeable medium bounded by a porous plate. This study also takes into account the effects of heat generation and absorption. The flow of the fluid is influenced by a consistent transverse magnetic field. The primary objective is to investigate the fluid's behavior under free convection while considering the impact of the Dufour effect and pressure. The nonlinear PDEs governing energy, momentum, and mass diffusion are worked out using the perturbation method and MATLAB coding. Graphical representations illustrate the modifications in velocity (u), temperature (θ) and concentration (ϕ) profiles across different parameters. Also, equations are derived for the skin friction (SF), Nusselt number (Nu) and Sherwood number (Sh).

1. INTRODUCTION

Heat transfer that occurs amid a moving fluid and a surface when they have different temperatures is called convection. Natural convection is created by buoyancy forces, which rises of density differences generated by temperature differences in the fluid. The impact of natural convection is encountered in transfer of mass. The discipline of electrically conducting liquid movement in the existence of a magnetic field is termed as magneto hydrodynamics (MHD). MHD delves into circumstances such as the generation of electric currents and magnetic fields through fluid motion (induction), along with the relationship between motion of fluid and magnetic fields. Its utilizations span across distinct fields, encompassing astrophysics, geophysics, engineering and plasma physics. Radiation is the process in which energy is released or transferred through space or a material substance in the form of waves. This energy manifests in diverse forms, encompassing electromagnetic radiation like radio waves, Xrays, light, microwaves and gamma rays, as well as particle radiation such as neutrons, alpha particles and beta particles. It holds significant importance across various domains, including natural processes, technological advancements like medical imaging and telecommunications and the operations of celestial bodies. Pressure is the force exerted on a surface per unit area, serving as a gauge for the concentration of force spread over a specific area. In the realm of physics, comprehending pressure is essential for analyzing phenomena in fluid dynamics, thermodynamics and mechanics. Its significance extends across a wide array of disciplines, encompassing engineering, meteorology, biology and chemistry.

In fluid dynamics, a chemical reaction denotes a sequence where chemical elements undergo changes, resulting in the generation of fresh chemical compounds or modifications to existing ones within a fluid environment. These chemical transformations within fluid dynamics are pivotal for comprehending a range of phenomena, including combustion, chemical kinetics and reactions in aqueous solutions. Furthermore, they hold substantial importance across disciplines such as engineering, environmental science and biophysics. Viscoelastic fluids are substances that demonstrate properties of both fluids and solids when subjected to deformation. In contrast to fluids that flow continuously under stress and solids that return to their original shape after stress removal, viscoelastic fluids display a blend of these behaviors. This unique characteristic allows them to deform under stress and partially recover once the stress is relieved. Viscoelastic fluids find widespread use across different fields, including polymers, biological tissues and specific fluids utilized in engineering and manufacturing processes. The Dufour effect (Df) is a thermodynamic phenomenon observed in fluid systems, particularly in mixtures of fluids or porous materials, where thermal diffusion and mass diffusion mutually influence one another. Specifically, it entails the generation of a temperature gradient within a fluid due to concentration gradients. This effect results from the interaction between HAMT and is significant in various natural and engineering scenarios, such as heat exchangers, combustion processes and the transport of substances in porous materials.

The Prandtl boundary-layer theory has been expanded to encompass an idealized elastico-viscous liquid. Numerical solutions have been derived for the equations of the boundary layer related to 2-D stream near a stagnation point. This analysis, done by Beard and Walter [1] reveals that elasticity predominantly augments velocity within the boundary layer and intensifies stress exerted on the solid boundary. Mishra et al. [2] examined the impact of HAMT on the free convective stream of an electrically conducting, incompressible fluid (ECIF) that is viscoelastic in nature via an upright porous plate within a permeable channel. The permeability and suction vary over time and oscillate, affected by both a heat source and a uniform perpendicular magnetic field. Ibrahim et al. [3] provided analytical solutions for the HAMT arising from the laminar flow of an electrically conducting, Newtonian and viscous fluid with heat generation or absorption on an erect permeable surface. These solutions consider the existence of radiation, mass flux and a first order homogeneous chemical process. Muthucurmaraswamy and Ganesan [4] numerically investigated the transient stream of an incompressible, viscous fluid via a semi-infinite thermal equilibrium plate subject to natural convection conditions. This solution considers the mass flux and a first-order homogeneous chemical reaction through the plate. Chamkha [5] presented analytical solutions for HAMT in the laminar stream of a Newtonian, electrically conducting, viscous fluid that generates or absorbs heat. The study investigates a vertically moving permeable surface influenced by a magnetic domain and a first-order chemical interaction.

Ali Chamkha [6] explored the unsteady, 2D, laminar boundary-layer flow of a viscous, ECIF that absorbs heat, along a half-infinite upright permeable moving plate. The situation includes a consistent crosswise magnetic influence and the buoyant forces of thermal and concentration changes. Santhosha et al. [7] researched the integrated consequences of radiation and chemicals on MHD free convective HAMT stream of viscous, elastic, ECIF via a permeable substance, enclosed by a porous plate, in the existence of heat generation or absorption. Choudhury and Das [8] carried out a study of free convective MHD visco-elastic fluid stream with HAMT over a vertically moving plate at a constant velocity, incorporating Df and Soret effects (Sr). The fluid is modelled as a non-Newtonian substance, specifically Walters liquid (Model B'). Perturbation techniques are utilized to resolve the equations governing the fluid flow and HAMT. Anusha et al. [9] examined the MHD convective flow of Walters-B memory liquid via a penetrable accelerating surface, incorporating the Sr and Df. The flow equation consists of a set of PDEs that describe the behavior of a non-Newtonian liquid. By employing appropriate similarity terms, the PDEs were simplified to ODEs. The study done by Zhao et al. [10] focuses on the unsteady natural convection HAMT of a MHD viscoelastic fluid in a permeable substance, incorporating Sr and Df. The equations of boundary layer, featuring coupled mixed time-space fractional derivatives, are worked out using a finite difference method in conjunction with the L1-algorithm.

Idowu and Falodun [11] examined the Sr-Df on MHD HAMT of Walter's-B visco-elastic fluid via a half-infinite erect plate. The equations of motion, a set of PDEs, are made dimensionless by introducing a suitable non-dimensional terms. These non-dimensional equations, alongside with the boundary conditions, are figured out numerically by the Spectral Relaxation Method (SRM), along with MATLAB R2012a. Sheri et al. [12] analyzed the influence of Hall current, Df and Sr on transient MHD flow via an inclined permeable plate. The fundamental non-linear PDEs are transformed into non dimensional non-linear PDEs using similarity transformations. The non-dimensional governing equations of

the study are worked out numerically by the Finite Element Method (FEM) with suitable initial conditions. Suneetha et al. [13] investigated the flow of a MHD viscoelastic fluid via a moving upright plate in a permeable substance, considering variable temperature and radiation effects. Additionally, chemical reactions and concentration are considered. The mathematical model is analytically addressed using a perturbation technique. Pal and Chatteriee [14] investigated MHD mixed convection, focusing on the integrated effects of Sr and Df on the HAMT of a power-law fluid via an slanted plate in a permeable medium. This study considers thermal radiation, changeable thermal conductivity, Ohmic dissipation, chemical reaction and suction/injection. Hayat et al. [15] examined the HAMT incorporating Sr and Df in the MHD 3-D flow of a second-grade fluid within a rotating reference frame. The homotopy analysis method is utilized to obtain a series solution. Nawaz et al. [16] investigated the Df and Sr on the steady, 2-D MHD flow of a viscous, electrically conducting fluid confined between infinite sheets. The permeable substance is filled with a viscous, incompressible fluid. The study includes the influences of Joule heating, viscous dissipation and a first-order chemical process.

Baag et al. [17] presented an in-depth theoretical study of unsteady MHD free convection flow of a visco-elastic fluid via a permeable substance, which is considered optically transparent and incompressible. The flow of the fluid is driven by the shearing force of a moving wall, with time-dependent suction. Radiative heat transfer is included in the equation of temperature. Ali et al. [18] examined the impact of slip conditions on the unsteady MHD flow of visco-elastic, incompressible fluids in a permeable substance, influenced by a cross magnetized region and Hall current, along with HAMT. The channel flow is driven by an oscillatory external pressure gradient. Sahoo [19] presented the transient flow of an viscoelastic ECIF modeled by the Walter B' model, with concurrent HAMT near an oscillating permeable plate in a slip-flow regime, influenced by a uniform crosswise magnetic zone. Kulkarni [20] investigated the non-steady flow of an elastico-viscous, ECIF via a permeable substance between two parallel plates, under the impact of a crosswise magnetized region. At the start, the stream is propelled by a consistent pressure variation that runs parallel to the enclosing liquids. After reaching a steady state, the variation in the pressure is swiftly removed. The subsequent motion of the fluid between the equidistant plates, influenced by a magnetic field, is then analyzed. Loganathan and Elamparithi [21] investigated the effects of chemical process, the Joule effect and heat sources or sinks on HAMT in MHD mixed convection flow via an infinite vertical plate, incorporating Ohmic heating and viscous dissipation. The work aims to include the Df and examined its impact alongside various parameters. Applying the homotopy analysis method (HAM) with two auxiliary parameters to investigate HAMT in a steady, 2-D MHD viscoelastic fluid stream over a stretching erect surface, considering the Sr and Df was done by Rashidi et al. [22]. The governing PDEs for the 2-D boundary layer are derived using the Boussinesq's approximation.

Dey and Borthakur [23] explored the HAMT characteristics of an elastico-viscous MHD fluid, modeled using Walter's B' formulation, as it flows through a porous medium. The flow is confined by an oscillating permeable plate within a slip-flow regime and is influenced by a uniform transverse magnetized region. The primary aim is to analyze the behavior of the fluid under forced convection while accounting for Df-Sr effects.

Pal and Saha [24] analyzed the influence of MHD effects on the flow of a temperature-dependent, viscous and chemically reactive thin fluid film past a non-steady, penetrable and stretchable plate. The analysis considers the influence of Sr-Df effects, non-linear thermal radiation, and suction, all within the framework of a convective boundary condition.

Sudarmozhi et al. [25] did a numerical analysis of MHD flow, radiation, activation energy, Sr and Df effects, and transfer of heat in a penetrable channel for a Maxwell fluid. The governing equations for momentum, concentration, and heat are converted into ODEs using a similarity transformation, facilitating a more focused and precise analysis. Understanding the behavior of non-Newtonian fluids in natural settings, such as rivers and groundwater flow, is crucial for assessing their environmental effect. The Sr and Df effects play a significant role in the transport of contaminants and heat within these systems. With this application in focus, Sudarmozhi et al. [26] explored the steady-state influence of radiation, Sr and Df on a permeable perpendicular plate using the Maxwell fluid model.

The current work investigates the influence of pressure, chemical reactions, Df, heat sources and radiation absorption on MHD free convective HAMT in a visco-elastic ECIF flowing via permeable medium surrounded by a permeable plate.

2. MATHEMATICAL FORMULATION

The appearance of magnetic field, radiation absorption, pressure, chemical reaction and heat generation in a 2D unsteady convective flow of visco-elastic fluid that is incompressible in nature and electrically conducting, passing through a semi-endless upright porous plate is explored here. In Figure 1, let 'x'-axis be considered through the permeable plate in the increasing track and standard to it is considered the 'y'-axis. It is supposed that applied voltage is absent in the flow, implying the lack of an electric field. The porous medium is supposed to be a plate filled with small, similar spherical pieces. Chemical reactions arise in the stream and physical attributes are thought to be consistent. The viscous and magnetic dissipations are negligible. All factors associated with stream, apart from pressure, were elements of 'y' and 't' because of the supposition that, the plate in the x - heading is of limitless length.

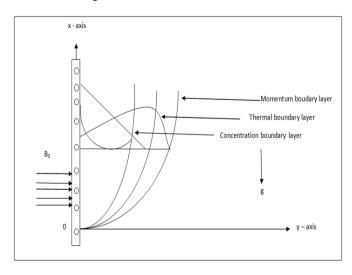


Figure 1. Configuration of the problem

3. PHYSICAL MODEL OF THE PROBLEM

By considering the Boussinesq's approximation, the controlling equations of the unsteady flow are represented as follows: The equation of continuity is expressed in Eq. (1), the equation of conservation of momentum is given in Eq. (2), the equation of energy is represented in Eq. (3), and the equation of transfer of mass is provided in Eq. (4).

$$\frac{\partial v}{\partial y} = 0 \tag{1}$$

$$\frac{\partial u}{\partial t} + v \frac{\partial u}{\partial y} = v \frac{\partial^2 u}{\partial y^2} - K_1' \frac{\partial^3 u}{\partial y^2 \partial t} + g\beta (T - T_\infty) + g\beta^* (C - C_\infty) - \frac{\sigma_e B_0^2}{\rho} u - \frac{v}{K_0} u - \frac{1}{\rho} \frac{\partial P}{\partial x}$$

$$\rho C_p \left(\frac{\partial T}{\partial t} + v \frac{\partial T}{\partial y} \right) = k \frac{\partial^2 T}{\partial y^2} - \frac{\partial q_r}{\partial y} - s' (T - T_\infty)$$
(2)

$$-R'(C-C_{\infty}) + \frac{D_{KT}}{C_{\infty}} \frac{\partial^2 C}{\partial y^2}$$
 (3)

$$\frac{\partial C}{\partial t} + v \frac{\partial C}{\partial y} = D \frac{\partial^2 C}{\partial y^2} - K' (C - C_{\infty})$$
 (4)

Boundary conditions (B.C):

$$u = U_0 (1 + \varepsilon e^{i\alpha t}), T = T_w + \varepsilon (T_w - T_\infty) e^{i\alpha t},$$

$$C = C_w + \varepsilon (C_w - C_\infty) e^{i\alpha t} \quad at \quad y = 0$$

$$u \to 0, T \to T_\infty, C \to C_\infty \text{ as } y \to \infty$$
(5)

Here U_0 is the plate velocity, T_w is the wall dimensional temperature, C_w is the wall dimensional concentration, T_∞ is the free stream dimensional temperature and C_∞ is the free stream dimensional concentration and ω – the constant.

From Eq. (1), the value of velocity is assumed as follows:

$$v = -V_0 \tag{6}$$

In Eq. (6), V_0 is the velocity of suction perpendicular to the plate.

The dimensional-less quantities are introduced as below:

$$y^{*} = \frac{U_{0}}{v} y; u^{*} = \frac{u}{U_{0}}; \theta = \frac{T - T_{\infty}}{T_{w} - T_{\infty}}; \phi = \frac{C - C_{\infty}}{C_{w} - C_{\infty}}; t^{*} = \frac{U_{0}^{2} t}{v};$$

$$V_{0}^{*} = \frac{V_{0}}{U_{0}}; Sc = \frac{v}{D}; K_{r} = \frac{K' v}{U_{0}^{2}};$$

$$M^{2} = \frac{\sigma_{e} B_{0}^{2} v}{\rho U_{0}^{2}}; Pr = \frac{\mu C_{p}}{k}; S = \frac{v^{2} S^{1}}{U_{0}^{2} k}; R_{1} = \frac{R^{1} v^{2} (C_{w} - C_{\infty})}{U_{0}^{2} k (T_{w} - T_{\infty})};$$

$$Gr = \frac{vg \beta (T_{w} - T_{\infty})}{U_{0}^{3}}; Gm = \frac{vg \beta^{*} (C_{w} - C_{\infty})}{U_{0}^{3}}; K_{p} = \frac{U_{0}^{2} K_{0}}{v^{2}};$$

$$\lambda_{1} = \frac{U_{0}^{2} K_{1}'}{v^{2} \rho}; Df = \frac{D_{KT} (C_{w} - C_{\infty})}{C_{s} C_{w} v (T_{w} - T_{\infty})}$$

The Eqs. (2)-(4) takes the upcoming form by applying the pre-mentioned non-dimensional values and Eq. (6).

$$\frac{\partial u}{\partial t} - V_0 \frac{\partial u}{\partial y} = \frac{\partial^2 u}{\partial y^2} + Gr\theta + Gm\phi - M_1 u$$

$$-\lambda_1 \frac{\partial^3 u}{\partial y^2 \partial t} - P \tag{8}$$

$$\Pr \frac{\partial \theta}{\partial t} - \Pr V_0 \frac{\partial \theta}{\partial y} = \frac{\partial^2 \theta}{\partial y^2} - (S + F)\theta$$

$$-R_1 \phi + Df \frac{\partial^2 \phi}{\partial y^2} \tag{9}$$

$$Sc\frac{\partial\phi}{\partial t} - ScV_0 \frac{\partial\phi}{\partial y} = \frac{\partial^2\phi}{\partial y^2} - ScKr\phi \tag{10}$$

where,
$$M_1 = M^2 + \frac{1}{K_n}$$
.

The corresponding B.C.s are,

$$u = 1 + \varepsilon e^{i\omega t}, \theta = 1 + \varepsilon e^{i\omega t}, \phi = 1 + \varepsilon e^{i\omega t} at y = 0$$

$$u \to 0, \theta \to 0, \phi \to 0 \text{ as } y \to \infty$$
(11)

4. SOLUTION OF THE PROBLEM

The perturbation method is a commonly employed analytical approach for solving nonlinear differential equations. It involves introducing a small parameter, known as the perturbation parameter, to transform complex problems into a sequence of solvable linear equations.

Let the governing equation of fluid velocity (u^*) , temperature (θ^*) and concentration (ϕ^*) fields be expressed as:

$$u*(y,t) = u_0(y) + \varepsilon u_1(y) e^{i\omega t}$$

$$\theta*(y,t) = \theta_0(y) + \varepsilon \theta_1(y) e^{i\omega t}$$

$$\phi*(y,t) = \phi_0(y) + \varepsilon \phi_1(y) e^{i\omega t}$$
(12)

Here, y is dependent variable, ε is a small perturbation parameter, Gr - thermal Grashof number, Gm - mass Grashof number, M - magnetic variable, $\lambda 1$ - viscoelastic variable, Pr - Prandtl number, S - heat absorption variable, R1 - radiation absorption parameter, Sc - Schmidt number, Kr - chemical reaction variable and F - Radiation parameter.

On substituting Eq. (12) in the Eqs. (8)-(10) and applying B.C.s (11), the solutions are obtained in terms of the perturbation parameter - ε . The expanded equations are grouped based on the powers of ε . By equating the similar terms and leaving out the terms of ε^2 the following equations are obtained.

Eqs. (8)-(10) takes the upcoming form by equating the similar terms and leaving out the terms of ε^2 and by substituting Eq. (12) on them.

$$u_0$$
"+ V_0u_0 '- M_1u_0 = $-Gr\theta_0 - Gm\phi_0 - P$ (13)

$$N_1 u_1 + V_0 u_1 - N_2 u_1 = -Gr\theta_1 - Gm\phi_1$$
 (14)

$$\theta_0$$
" + $\Pr V_0 \theta_0$ ' - $(S + F) \theta_0 = R_1 \phi_0 - Df \phi_0$ " (15)

$$\theta_1 "+ \Pr V_0 \theta_1 '- \left(S + F + i \Pr \omega\right) \theta_1 = R_1 \phi_1 - Df \phi_1 " \qquad (16)$$

$$\phi_0$$
 "+ $ScV_0\phi_0$ '- $ScKr\phi_0 = 0$ (17)

$$\phi_1 " + ScV_0 \phi_1 ' - Sc(Kr + i\omega)\phi_1 = 0$$
 (18)

Here,
$$N_1 = 1 - i\lambda_1 \omega$$
, $N_2 = M_1 + i\omega$.

In these equations prime notation denotes the differentiation of terms regarding "y".

The corresponding B.C are:

$$u_{0} = 1, u_{1} = 1, \theta_{0} = 1, \theta_{1} = 1, \phi_{0} = 1, \phi_{1} = 1 \text{ at } y = 0,$$

$$u_{0} \to 0, u_{1} \to 0, \theta_{0} \to 0, \theta_{1} \to 0, \phi_{0} \to 0,$$

$$\phi_{1} \to 0 \text{ as } y \to \infty$$
(19)

Resolving the Eqs. (13)-(18), by applying Eq. (19) the following results are obtained:

$$u_0(y) = b * e^{m_{10}y} + b_7 e^{m_6 y} + b_8 e^{m_2 y} + b_9 e^{m_2 y} + b_{10} e^{0 y}$$
(20)

$$u_1(y) = b^{**}e^{m_{12}y} + b_{11}e^{m_8y} + b_{12}e^{m_4y} + b_{13}e^{m_4y}$$
 (21)

$$\theta_0(y) = (1 - b_3)e^{m_6 y} + b_3 e^{m_2 y} \tag{22}$$

$$\theta_{1}(y) = (1 - b_{6})e^{m_{8}y} + b_{6}e^{m_{4}y}$$
(23)

$$\phi_0(y) = e^{m_2 y} \tag{24}$$

$$\phi_{1}(y) = e^{m_{4}y} \tag{25}$$

By applying the expressions of u_0 , u_1 , θ_0 , θ_1 , ϕ_0 and ϕ_1 in the governing Eq. (12), the equations for u, θ and ϕ were obtained as below:

$$u*(y,t) = b*e^{m_{10}y} + b_{7}e^{m_{6}y} + b_{8}e^{m_{2}y} + b_{9}e^{m_{2}y} + b_{10}e^{0y} + \mathcal{E}e^{i\omega t}(b**e^{m_{12}y} + b_{11}e^{m_{8}y} + b_{12}e^{m_{4}y} + b_{13}e^{m_{4}y})$$
(26)

$$\theta^*(y,t) = (1-b_3)e^{m_6y} + b_3e^{m_2y} + \varepsilon e^{i\omega t}$$

$$((1-b_6)e^{m_8y} + b_6e^{m_4y})$$
(27)

$$\phi^*(y,t) = e^{m_2 y} + \varepsilon e^{i\omega t} e^{m_4 y} \tag{28}$$

Skin friction (SF):

The coefficient of rate of velocity is written as:

$$\tau = -\left(\frac{\partial u}{\partial y}\right)_{y=0} = -b * m_{10} - b_7 m_6 - b_8 m_2 - b_9 m_2 -$$

$$\varepsilon e^{i\omega t} \left(b * m_{12} + b_{11} m_8 + b_{12} m_4 + b_{13} m_4\right)$$
(29)

Nusselt number (Nu):

The coefficient of rate of transfer of heat is expressed as:

$$Nu = -\left(\frac{\partial \theta}{\partial y}\right)_{y=0}$$

$$= -\left(\left(1 - b_3\right)m_6 + b_3m_2 + \varepsilon e^{i\omega t}\left(\left(1 - b_6\right)m_2 + b_6m_4\right)\right)$$
(30)

Sherwood number (Sh):

The coefficient of rate of transfer of mass is specified as:

$$Sh = -\left(\frac{\partial \phi}{\partial y}\right)_{y=0} = -\left(m_2 + \varepsilon e^{i\omega t} m_4\right) \tag{31}$$

In the following work VP implies velocity profile, TP implies temperature profile and CP imply concentration profile.

5. RESULTS AND DISCUSSION

Figure 2 implies velocity increases as Df rises. The Df quantifies the influence of thermal diffusion on mass flux. When the Df increases, the thermal diffusion effect becomes more pronounced. This results in larger temperature gradients, which enhance buoyancy forces and convective currents. Consequently, these factors together cause an upsurge in the velocity of the fluid. Mechanism analysis: The Dufour number (Df) quantifies the energy flux generated by mass diffusion in a multi component fluid. As Df increases, the influence of concentration gradients on thermal energy flux intensifies. This additional energy input affects flow dynamics, promoting fluid motion. Higher Df values strengthen the interaction between thermal energy and fluid flow, directly influencing the fluid's movement.

Figure 3 shows velocity rises as pressure increases. It is because when pressure increases, it can accelerate the fluid, thereby increasing its velocity. This phenomenon occurs due to the unique stress-strain responses of viscoelastic fluids in the existence of a magnetic field. Mechanism analysis: As pressure rises, the force acting on fluid particles intensifies, leading to greater momentum and an increase in velocity. This behavior is explained by the Navier-Stokes equations, which describe fluid motion by accounting for pressure, viscosity, and external forces. In viscoelastic fluids, higher pressure enhances deformation due to their elastic properties, enabling efficient energy storage and release. As a result, these fluids achieve higher velocities when exposed to a pressure gradient.

Figure 4 shows velocity diminishes with rise in magnetic variable, as the transverse magnetic forces reduce the velocity. Mechanism analysis: In an electrically conducting fluid, the interaction between the magnetized region (B_0) and the induced electric current generates a Lorentz force. This force resists the fluid's motion, acting as a resistive force that slows down the flow. Near boundaries, such as walls, this effect becomes more significant due to the stronger interrelation between the magnetic field and the induced currents. The primary impact of the Lorentz force is the reduction of kinetic energy in the fluid as a consequence of magnetic forces. The decline in velocity with increasing M highlights the role of the Lorentz force as a resistive mechanism in MHD flows, which can be leveraged in various engineering applications.

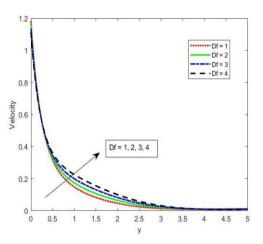


Figure 2. Df on VP

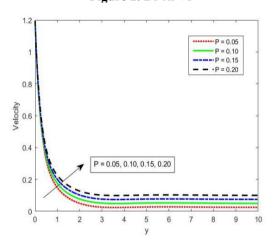


Figure 3. P on VP

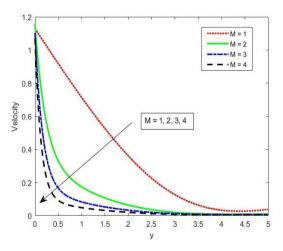


Figure 4. M on VP

Figure 5 implies the velocity decreases as there is a boom in Kr. An increase in Kr accelerates the rate of concentration changes. Additionally, a rise in Kr enhances mass diffusion, which introduces extra resistance to the flow, resulting in a reduction in velocity. Mechanism analysis: The chemical reaction parameter (Kr) quantifies the rate of a chemical reaction within the flow, with higher values indicating faster reaction rates. An increase in Kr enhances mass diffusion, which influences fluid properties by driving species transport due to concentration gradients. This intensified diffusion creates additional resistance to fluid motion, as momentum transfer is affected by the interaction between species

concentration and velocity. The coupling between chemical reactions and diffusion alters the boundary layer thickness, with a higher Kr typically causing a thicker concentration boundary layer. This results in a reduced velocity gradient near the surface, ultimately contributing to a decrease in overall fluid velocity.

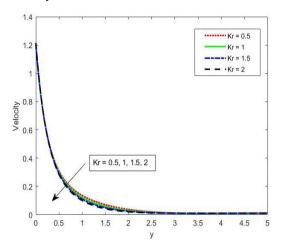


Figure 5. Kr on VP

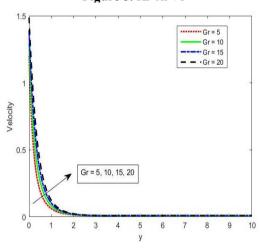
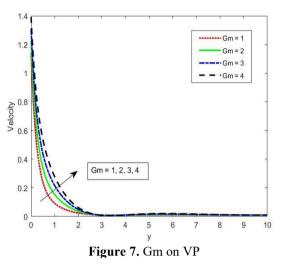


Figure 6. Gr on VP

Figures 6 and 7 implies when Gr and Gm rises, velocity increases. As the thermal Grashof number enhances, buoyant forces become more dominant than viscous forces, leading to stronger convective flow and increased fluid velocities. This phenomenon is a fundamental characteristic of buoyancydriven (free convection) flows, where temperature gradients create density differences, resulting in higher flow velocities in warmer regions. Mechanism analysis: Gr and Gm quantify the ratio of buoyant forces arising from temperature and concentration differences, respectively, to viscous forces. As the values of Gr or Gm escalates: the dominance of buoyant forces over viscous forces becomes more pronounced; viscous forces become insufficient to counteract buoyancy-induced acceleration, resulting in enhanced fluid velocity; greater temperature gradients surge buoyant effects, intensifying fluid movement; larger concentration gradients generate solutal buoyancy, which reinforces thermal buoyancy, further accelerating the flow.

Higher Pr indicates lower thermal diffusivity and higher momentum diffusivity. This results in weaker buoyancy forces due to diminished temperature gradients and greater viscous resistance from steeper velocity gradients, which ultimately decreases the flow velocity and is depicted in Figure 8. Mechanism analysis: The Pr represents the ratio of momentum diffusivity (kinematic viscosity) to thermal transfer rate. A higher Pr implies momentum diffusivity is more dominant than thermal diffusivity, meaning heat diffuses more slowly than momentum within the fluid. In fluids with a high Pr, such as oils and glycerin, low thermal diffusivity results in weaker buoyancy forces and increased viscous resistance, ultimately reducing the flow velocity.



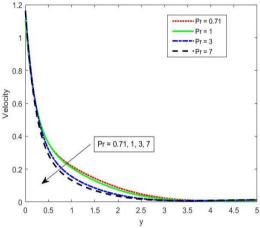


Figure 8. Pr on VP

As the Sc boosts up, the velocity falls off because higher Sc are associated with lower mass diffusivity and higher momentum diffusivity. It is well depicted in Figure 9. Mechanism analysis: The Sc represents the ratio of momentum transfer rate to mass diffusivity. A higher Sc denotes greater momentum diffusivity, which amplifies the influence of viscous forces. Increased viscous resistance results in steeper velocity gradients within the boundary layer. As a consequence, the intensified viscous effects hinder fluid motion, leading to a reduction in overall velocity.

Figure 10 implies as the radiation parameter rises, the velocity declines due to greater heat loss through thermal radiation. This reduces the temperature gradient and consequently, the buoyancy forces driving the flow. The weakened buoyancy forces result in lower fluid velocities. Mechanism analysis: The radiation parameter (R) quantifies the relative influence of radiative transfer of heat compared to thermal conduction. A higher R indicates increased energy loss from the system due to thermal radiation. Since buoyancy forces depend on temperature differences, a reduced

temperature gradient weakens the driving force for fluid motion. As buoyancy forces decrease, the fluid's capability to counteract viscous resistance declines, causing lower flow velocities. The interaction between radiation and buoyancy plays an important role in varied engineering and environmental applications.

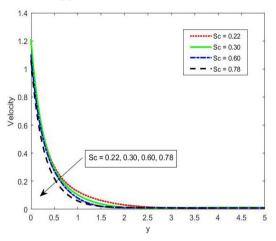


Figure 9. Sc on VP

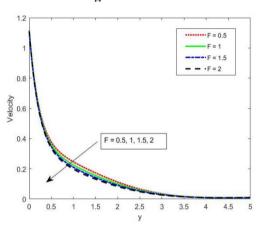


Figure 10. F on VP

As the viscoelastic parameter escalates, the velocity rises because the fluid's elastic properties enhance its ability to recover and sustain motion. The reduction in viscous drag combined with the aid of elastic recovery in driving the flow leads to higher fluid velocities and is represented in Figure 11. Mechanism analysis: The viscoelastic parameter measures the extent to which elastic effects influence fluid behavior relative to viscosity. Elastic forces introduce additional momentum into the flow, helping to counteract viscous resistance and resulting in increased velocities.

Figure 12 shows as Df increases, the temperature rises because the Df enhances heat transfer due to concentration gradients. This additional heat flux raises the overall temperature of the fluid. The coupling of HAMT processes through the Df leads to higher fluid temperatures when the Df is significant. Mechanism analysis: The Df represents the impact of mass diffusion on heat transfer of heat within the flow. As Df increases, concentration gradients contribute to additional heat flux, facilitating greater thermal energy transfer throughout the fluid. A higher Df strengthens the interaction between concentration gradients and heat transfer, resulting in an overall rise in fluid temperature.

As the Sc increases, the temperature rises due to lower mass diffusivity. This results in less efficient mixing and more

pronounced concentration gradients, which lead to increased localized heating via the Df. The reduced mass diffusion enhances thermal energy retention in areas with significant concentration gradients, thereby raising the overall temperature of the fluid. This is shown in Figure 13. Mechanism analysis: As Sc escalates, mass diffusivity decreases, leading to less efficient mixing of concentration gradients. This diminished ability to uniformly diffuse solutes results in sharper concentration gradients in regions where solutal effects are prominent. Areas with significant concentration gradients experience increased thermal energy retention, driven by the additional heat flux induced by the Dufour effect.

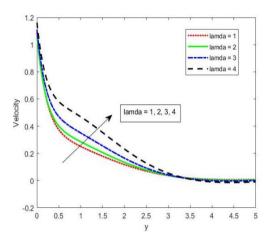


Figure 11. Lamda on VP

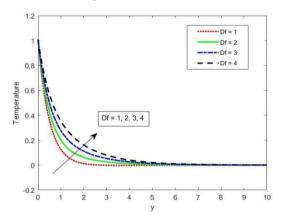


Figure 12. Df on TP

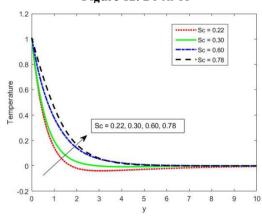


Figure 13. Sc on TP

Figure 14 displays, as the Pr rises, the temperature declines because a higher Pr corresponds to lower thermal diffusivity.

This results in less efficient heat conduction away from the heated surface, confining the heat to a thinner boundary layer and reducing the overall temperature rise within the fluid. The reduced thermal diffusivity lowers temperatures in the bulk fluid, despite the increased convective efficiency near the plate. Mechanism analysis: A higher Pr implies lower thermal diffusivity, which decreases the efficiency of heat conduction away from the heated surface. This reduction in thermal diffusion, combined with localized heat confinement, leads to a general fall in temperature throughout the fluid.

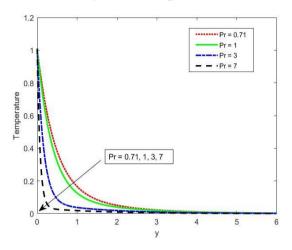


Figure 14. Pr on TP

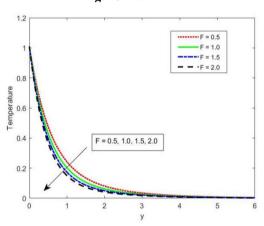


Figure 15. F on TP

As the radiation parameter rises, the temperature decreases due to greater radiative heat loss. This enhanced heat loss reduces the thermal energy retained in the fluid, resulting in a reduction of overall temperature of the fluid. Increased radiation effectively cools the fluid, leading to a temperature decrease as the radiation parameter rises. This is shown in Figure 15. Mechanism analysis: As the radiation parameter increases, a greater amount of thermal energy is released to the surroundings, causing a decline of the overall fluid temperature.

Figure 16 shows as the chemical reaction parameter enhances the concentration of the fluid decreases because a higher parameter corresponds to a faster consumption rate of the species. This accelerated reaction rate results in quicker depletion of the species, leading to a lower overall concentration within the fluid. The increased consumption caused by the chemical reaction significantly reduces the concentration levels as the reaction parameter boosts up. Mechanism analysis: Kr measures the rate at which a chemical species is consumed or produced due to reactions within the

fluid. A higher Kr indicates an increase in the reaction rate, resulting in faster consumption of the reacting species. This accelerated reaction rate causes a more rapid decline in the concentration of the reacting species, particularly in areas close to the reaction zones.

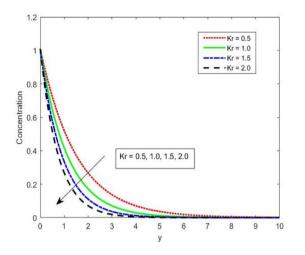


Figure 16. Kr on CP

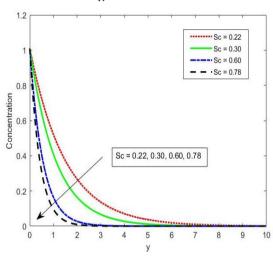


Figure 17. Sc on CP

Table 1. Numerical values of SF, Nu and Sh for distinct parameters

				•			
P	Df	M	Kr	λ	τ	Nu	Sh
0.05	1	2	0.5	1	3.1551	2.1755	0.6647
0.10	1	2	0.5	1	3.0400	2.1755	0.6647
0.15	1	2	0.5	1	2.9248	2.1755	0.6647
0.20	1	2	0.5	1	2.8097	2.1755	0.6647
0.05	1	2	0.5	1	3.1551	2.1755	0.6647
0.05	2	2	0.5	1	3.0517	1.8532	0.6647
0.05	3	2	0.5	1	2.9482	1.5308	0.6647
0.05	4	2	0.5	1	2.8447	1.2085	0.6647
0.05	1	1	0.5	1	0.6945	2.1755	0.6647
0.05	1	2	0.5	1	3.1551	2.1755	0.6647
0.05	1	3	0.5	1	5.2352	2.1755	0.6647
0.05	1	4	0.5	1	7.1704	2.1755	0.6647
0.05	1	2	0.5	1	3.1551	2.1755	0.6647
0.05	1	2	1	1	3.1066	2.1755	0.8869
0.05	1	2	1.5	1	3.0638	2.1755	1.1090
0.05	1	2	2	1	3.0258	2.1755	1.3312
0.05	1	2	0.5	1	3.1551	2.1755	0.6647
0.05	1	2	0.5	2	3.1508	2.1755	0.6647
0.05	1	2	0.5	3	3.1492	2.1755	0.6647
0.05	1	2	0.5	4	3.1483	2.1755	0.6647

Table 2. Numerical values of SF, Nu and Sh for distinct parameters

Gr	Gm	Pr	Sc	F	τ	Nu	Sh
5	1	0.71	0.22	0.5	3.1551	2.1755	0.6647
10	1	0.71	0.22	0.5	2.1106	2.1755	0.6647
15	1	0.71	0.22	0.5	1.0660	2.1755	0.6647
20	1	0.71	0.22	0.5	0.0214	2.1755	0.6647
5	1	0.71	0.22	0.5	3.1551	2.1755	0.6647
5	2	0.71	0.22	0.5	2.8477	2.1755	0.6647
5	3	0.71	0.22	0.5	2.5403	2.1755	0.6647
5	4	0.71	0.22	0.5	2.2328	2.1755	0.6647
5	1	0.71	0.22	0.5	3.1551	2.1755	0.6647
5	1	1.00	0.22	0.5	3.2483	2.6364	0.6647
5	1	3.00	0.22	0.5	3.6455	6.3173	0.6647
5	1	7.00	0.22	0.5	3.9077	14.1964	0.6647
5	1	0.71	0.22	0.5	3.1551	2.1755	0.6647
5	1	0.71	0.30	0.5	3.1025	1.9338	0.9064
5	1	0.71	0.60	0.5	2.9562	1.0357	1.8129
5	1	0.71	0.78	0.5	2.8940	0.5041	2.3567
5	1	0.71	0.22	0.5	3.1551	2.1755	0.6647
5	1	0.71	0.22	1.0	3.1893	2.3377	0.6647
5	1	0.71	0.22	1.5	3.2184	2.4852	0.6647
5	1	0.71	0.22	2.0	3.2439	2.6213	0.6647

As the Sc boosts up, the concentration of the fluid reduces because a boosted Sc leads to reduced mass diffusivity. This reduced diffusivity results in slower mixing and spreading of the species, creating a steeper concentration gradient and lower overall concentration levels in the fluid and is well depicted in Figure 17. Mechanism analysis: As the Sc increases, the rate of mass diffusion decreases, which slows the mixing and spreading of chemical species within the fluid. The overall concentration diminishes because the diffusion process, responsible for species transport, is considerably reduced.

The specified parameter values are used for computations unless stated otherwise in Table 1 and Table 2: P=0.05, $\epsilon=0.01$, $\omega=2$, $\lambda=1$, t=0.1, Gr=5, Gr=1, Kp=3, M=2, V0=2, R1=0.5, Pr=0.71, S=1, F=0.5, Kr=0.5, S=0.22, Df=1.

6. CONCLUSION

In the present study, pressure, chemical reaction, heat source, Dufour effect and radiation absorption on MHD free convective HAMT flow of electrically conducting, viscous, incompressible, visco-elastic liquid passing by a permeable medium surrounded by permeable plate were explored. The governing equations in their non-dimensional form are worked out using the perturbation technique, with conclusions presented through graphs and tables. The outcomes can be summarized as follows:

- i. The increase in Df influences energy transport by enhancing thermal energy transfer through mass diffusion. This modifies fluid characteristics leading to higher VP. As Df increases, the VP exhibit a notable increase both near the wall and across the entire domain, confirming the strong interaction between thermal diffusion effects and fluid flow dynamics.
- ii. An increase in pressure gradient boosts the overall energy of the flow, intensifying buoyancy-driven currents. This leads to rise in VP. The increase in velocity of viscoelastic fluids under rising pressure within a magnetic field is influenced by the combined effects of

- pressure gradient-driven acceleration, viscoelastic deformation, magnetohydrodynamic forces, and the fluid's inherent stress-strain behavior.
- iii. As Gr increases, the VP rises due to the greater temperature difference amplifying buoyancy forces. Also, the VP increases as Gm rises due to stronger solutal buoyancy forces generated by larger concentration differences. These forces overpower viscous resistance, enhancing the flow's efficiency. This phenomenon occurs in natural convection systems, including heat exchangers, environmental flows, and industrial cooling processes.
- iv. As the viscoelastic parameter rises, the fluid's VP increases due to reduced viscous resistance, improved responsiveness to buoyancy forces, diminished magnetic damping effects and altered boundary layer dynamics. Viscoelastic fluids are utilized in applications that demand reduced drag and smoother flow. They are also commonly used in polymer processing.
- v. The VP decreases with an upsurge in M due to the Lorentz force, which resists fluid motion and acts as a retarding force. This concept is applied in engineering for regulating fluid flow in electromagnetic pumps, minimizing turbulence, and stabilizing flows in heat transfer systems.
- vi. The rise in Kr results in a fall in VP because of the reduction in solutal buoyancy forces, changes in fluid properties and alterations in boundary layer dynamics. The interaction between chemical reactions, diffusion, and flow dynamics is fundamental for understanding and anticipating the behavior of such systems.
- vii. As Pr enhances, the VP decreases due to the lower thermal diffusivity and higher momentum diffusivity. This combination weakens the buoyancy force driving the flow and enhances viscous resistance leading to reduced fluid velocity. The interrelation between thermal and momentum diffusivity plays an important role in systems such as heat exchangers, industrial cooling, and natural convection flows.
- viii. The VP diminishes as Sc boosts up due to the reduced mass diffusivity, which weakens the solutal buoyancy forces driving the flow. This phenomenon is essential for understanding mass transfer flows, particularly in chemical reactors and environmental transport processes.
- ix. An increase in F, reduces the VP due to enhanced heat loss through radiative transfer, which weakens the thermal buoyancy forces driving the flow. This effect plays a crucial role in engineering and environmental systems, such as radiative heat transfer in furnaces and solar collectors, as well as atmospheric flows where radiative cooling influences convection.
- x. As Df rises, the TP rises because of enhanced heat generation through mass diffusion within the system. Df plays a vital role in systems involving HAMT, including chemical reactors and combustion processes. Natural phenomena like ocean currents and atmospheric flows also demonstrate the coupling of HAMT.
- xi. The TP rises as Sc hikes. It is due to slower mass diffusion, which results in a thicker concentration boundary layer and amplifies the influence of heat transfer. This concept is applied in oceanic and atmospheric systems, where high Sc fluids retain heat in localized regions due to steep concentration gradients.
- xii. The TP declines as F hikes. It is because, as F rises it

- leads to stronger radiative heat transfer which enhances heat loss from the fluid to the surroundings. This concept is applicable to atmospheric and astrophysical flows, where radiative heat transfer has a significant impact on temperature distributions.
- xiii. As Pr increases, the TP decreases since an enhanced Pr indicates that the fluid is more viscous compared to its thermal diffusivity. This leads to a drop in fluid temperature. This behavior is crucial in systems that require controlled heat transfer, such as cooling in high-viscosity fluid flows. The concept is relevant to high Pr gases in atmospheric systems, where temperature gradients are closely confined.
- xiv. The CP declines with rise in Kr. A higher Kr indicates a stronger chemical reaction that consumes or transforms the species in the fluid. It leads to lower CP. This application is found in industrial chemical processes, environmental systems, and biological systems.
- xv. An elevated Sc indicates diminished mass diffusivity, which leads to a thicker concentration boundary layer and slower mass transfer. Hence CP decreases. In chemical reactors, a higher Sc suggests that effective mixing strategies are required to maintain uniform concentration levels.
- xvi. The conclusions of the present work can be used in various fields such as nuclear reactor cooling systems, solar collectors and heat exchangers, petroleum industry, environmental engineering, biomedical engineering, chemical engineering, space technology and aerospace engineering and material processing.
- xvii. Future studies can investigate different analytical techniques, including the Finite Element Method and the Finite Volume Method. Moreover, the research scope can be broadened to incorporate a comparative evaluation of these methods.

REFERENCES

- [1] Beard, D.W., Walters, K. (1964). Elastico-viscous boundary layer flow, I. two dimensional flow near a stagnation point. Matematical Proceedings of the Cambridge Philosophical Society, 60(3): 667-674. https://doi.org/10.1017/S0305004100038147
- [2] Mishra, S.R., Dash, G.C., Acharya, M. (2013). Mass and heat transfer effect on MHD flow of a visco-elastic fluid through porous medium with oscillatory suction and heat source. International Journal of Heat and Mass Transfer, 57(2): 433-438. https://doi.org/10.1016/j.ijheatmasstransfer.2012.10.053
- [3] Ibrahim, F.S., Elaiw, A.M., Bakr, A.A. (2008). Effect of the chemical reaction and radiation absorption on the unsteady MHD free convection flow past a semi-infinite vertical permeable moving plate with heat source and suction. Communications in Non-linear Science and Numerical Simulation, 13(6): 1056-1066. https://doi.org/10.1016/j.cnsns.2006.09.007
- [4] Muthucumaraswamy, R., Ganesan, P. (2001). Effect of the chemical reaction and injection on flow characteristics in an unsteady upwards motion of an isothermal plate. Journal of Applied Mechanics and Technical Physics, 42: 665-71. https://doi.org/10.1023/A:1019259932039
- [5] Chamkha, J. (2003). MHD flow of a uniformly stretched

- vertical permeable surface in the presence of heat generation/absorption and a chemical reaction. International Communications in Heat and Mass Transfer, 30(3): 413-422. https://doi.org/10.1016/S0735-1933(03)00059-9
- [6] Ali Chamkha, J. (2004). Unsteady MHD convective heat and mass transfer past a semi-infinite vertical permeable moving plate with heat absorption. International Journal of Engineering Science, 42(2): 217-230. https://doi.org/10.1016/S0020-7225(03)00285-4
- [7] Santhosha, B., Younus, S., Kamala, G., Ramana Murthy, M.V. (2017). Radiation and chemical reaction effects on MHD free convective heat and mass transfer flow of a viscoelastic fluid past a porous with heat generation/ absorption. International Journal of Chemical Sciences, 15(3): 170.
- [8] Choudhury, R., Das, S.K. (2013). Visco-elastic MHD fluid flow over a vertical plate with Dufour and Soret effects. International Journal of Scientific & Engineering Research, 4(7): 11-17.
- [9] Anusha, P., NagaSwapnaSri, M., Venu Madhav, V.V., Chaitanya, C.S., Saxena, K.K., Abdul-Zahra, D.S., Linul, E., Spandana, V.V., Prakash, C., Budhi, D., Campilho, R. (2022). Dynamics of MHD convection of Walters B Viscoelastic fluid through an accelerating permeable surface using the Soret-Dufour mechanism. Applied Sciences, 12(19): 9431. https://doi.org/10.3390/app12199431
- [10] Zhao, J.H., Zheng, L.C., Zhang, X.X., Liu, F.W. (2016). Convection heat and mass transfer of fractional MHD Maxwell fluid in a porous medium with Soret and Dufour effects. International Journal of Heat and Mass Transfer, 103: 203-210. https://doi.org/10.1016/j.ijheatmasstransfer.2016.07.057
- [11] Idowu, A.S., Falodun, B.O. (2019). Soret—Dufour effects on MHD heat and mass transfer of Walter's-B viscoelastic fluid over a semi-infinite vertical plate: Spectral relaxation analysis. Journal of Taibah University for Science, 13(1): 49-62. https://doi.org/10.1080/16583655.2018.1523527
- [12] Sheri, S.R., Megaraju, P, Rajashekar, M.N. (2022). Impact of Hall Current, Dufour and Soret on transient MHD flow past an inclined porous plate: Finite element method. Materials Today: Proceedings, 59: 1009-1021. https://doi.org/10.1016/j.matpr.2022.02.279
- [13] Suneetha, K., Ibrahim, S.M., Reddy, G.V.R., Kumar, P.V. (2020). Variable temperature and concentration impacts on radiative chemically magnetohydrodynamic viscoelastic fluid flow through porous moving plate. Mathematical Modelling of Engineering Problems, 7(2): 187-195. https://doi.org/10.18280/mmep.070203
- [14] Pal, D., Chatterjee, S. (2013). Soret and Dufour effects on MHD convective heat and mass transfer of a power-law fluid over an inclined plate with variable thermal conductivity in a porous medium. Applied Mathematics and Computation, 219(14): 7556-7574. https://doi.org/10.1016/j.amc.2012.10.119
- [15] Hayat, T., Naz, R., Asghar, S. Alsaedi, A. (2014). Soret-Dufour effects on MHD rotating flow of a viscoelastic fluid. International Journal of Numerical Methods for Heat & Fluid Flow, 24(2): 498-520. https://doi.org/10.1108/HFF-03-2012-0076
- [16] Nawaz, M., Hayat, T., Alsedi, A. (2012). Dufour and Soret effects on MHD flow of viscous fluid between

- radially stretching sheets in porous medium. Applied Mathematics and Mechanics, 33: 1403-1418. https://doi.org/10.1007/s10483-012-1632-6
- [17] Baag, S., Acharya, M.R., Mishra, S.R., Dash, G.C. (2015). MHD flow of a visco-elastic fluid through a porous medium between infinite parallel plates with time dependent suction. Journal of Hydrodynamics, 27: 738-747. https://doi.org/10.1016/S1001-6058(15)60536-4
- [18] Ali, F., Khan, I., Samiulhaq, Mustapha, N., Shafie, S. (2012). Unsteady magnetohydrodynamic oscillatory flow of viscoelastic fluids in a porous channel with heat and mass transfer. Journal of the Physical Society of Japan, 81(6): 064402. https://doi.org/10.1143/JPSJ.81.064402
- [19] Sahoo, S.N. (2013). Heat and mass transfer effect on MHD flow of a viscoelastic fluid through a porous medium bounded by an oscillating porous plate in slip flow regime. International Journal of Chemical Engineering, 2013: 380679. http://doi.org/10.1155/2013/380679
- [20] Kulkarni, S.B. (2015). Unsteady MHD flow of elasticoviscous incompressible fluid through a porous medium between two parallel plates under the influence of a magnetic field. Defence Science Journal, 65(2): 119-125. http://doi.org/10.14429/dsj.65.7958
- [21] Loganathan, A., Elamparithi, S. (2023). MHD heat and mass transfer steady flow of a convective fluid through a porous plate in the presence of multiple parameters along with Dufour effect. International Journal of Heat and Technology, 41(1): 205-212. https://doi.org/10.18280/ijht.410122
- [22] Rashidi, M.M., Ali, M., Rostami, B., Rostami, P., Xie, G.N. (2015). Heat and mass transfer for MHD viscoelastic fluid flow over a vertical stretching sheet with considering Soret and Dufour effects. Mathematical Problems in Engineering, 2015: 861065. http://doi.org/10.1155/2015/861065
- [23] Dey, D., Borthakur, A. (2025). Heat and mass transfer of elastico-viscous MHD fluid flow through a porous medium bounded by an oscillating porous plate in slipflow regime under Soret and Dufour effects. Heat Transfer, 54(1): 646-669. https://doi.org/10.1002/htj.23187
- [24] Pal, D., Saha, P. (2024). Impact of variable viscosity, thermal conductivity, and Soret–Dufour effects on MHD radiative heat transfer in thin reactive liquid films past an unsteady permeable expandable sheet. Heat Transfer, 53(7): 3432-3459. https://doi.org/10.1002/htj.23096
- [25] Sudarmozhi, K., Iranian, D., Alessa, N. (2024). Viscoelastic fluid, flow on channel in porous medium with Soret and Dufour along with the effect of activation energy and suction and blowing. Journal of Taibah University for Science, 18(1): 2328869. https://doi.org/10.1080/16583655.2024.2328869
- [26] Sudarmozhi, K., Iranian, D., Khan, I., Hajjej, F., Omer,

A.S.A., Altayyar, F.A. (2024). Heat generation in dual convection Non-Newtonian MHD Darcy's flow with Soret and Dufour effects. Case Studies in Thermal Engineering, 53: 103704. https://doi.org/10.1016/j.csite.2023.103704

NOMENCLATURE

B_0	Magnetic field strength
g	Acceleration due to gravity
M	Magnetic variable
λ_1	Viscoelastic variable
Df	Dufour number
K_0	Permeability of the porous medium
Кp	Porosity parameter
D_{Kt}	Dufour coefficient
Ср	Specific heat at constant pressure
Cs	Concentration susceptibility
D	Chemical molecular diffusivity
F	Radiation parameter
Gm	Mass Grashof number
Gr	Thermal Grashof number
K_1	Viscosity related parameter
s'	Heat source parameter
R'	Reaction rate constant
K'	Chemical reaction parameter
Kr	Chemical reaction variable
k	Thermal conductivity
q_r	Radiative heat flux
R_1	Radiation absorption parameter
Nu	Local Nusselt number along the heat
	source
P	Pressure
Pr	Prandtl number
Sc	Schmidt number
S	Heat absorption variable
S^1	Specific heat absorption variable

Magnetia field strongth

Greek symbols

σ_{e}	Electrical conductivity
β	Thermal expansion coefficient
β*	Solute expansion coefficient
ρ	Fluid density
μ	Dynamic viscosity
ν	Kinematic viscosity

Subscripts

Temperature at the stationary plate
Temperature of the free flowing fluid
Concentration at the stationary plate
Concentration of the free flowing fluid